



Universality of the Momentum Band Density of Periodic Networks

Ram Band^{1,*} and Gregory Berkolaiko^{2,†}

¹*Department of Mathematics, Technion–Israel Institute of Technology, Haifa 32000, Israel*

²*Department of Mathematics, Texas A&M University, College Station, Texas 77843-3368, USA*

(Received 22 April 2013; published 24 September 2013)

The momentum spectrum of a periodic network (quantum graph) has a band-gap structure. We investigate the relative density of the bands or, equivalently, the probability that a randomly chosen momentum belongs to the spectrum of the periodic network. We show that this probability exhibits universal properties. More precisely, the probability to be in the spectrum does not depend on the edge lengths (as long as they are generic) and is also invariant within some classes of graph topologies.

DOI: [10.1103/PhysRevLett.111.130404](https://doi.org/10.1103/PhysRevLett.111.130404)

PACS numbers: 03.65.-w, 73.21.Hb

The spectrum of a Schrödinger operator in a periodic medium is calculated using the Floquet-Bloch procedure [1]: the periodic medium is replaced with its fundamental domain endowed with parameter-dependent quasiperiodic boundary conditions. The resulting parameter-dependent spectrum is called the dispersion relation, and the range of the dispersion relation is precisely the spectrum of the original structure. The spectrum has a band-gap structure, and knowing the band location and sizes is of utmost importance in the theories of condensed matter and of dielectric and acoustic media [2–6]. Of particular recent interest is understanding the spectrum of quantum graphs [7,8], motivated by their applications to solid state physics [9,10], photonic crystals [11], carbon nanostructures [12], as well as their use as models for quantum chaos, both in theoretical [13–18] and experimental [19,20] studies.

In the present Letter, we explore the *relative* size of bands and gaps and discover a curious universality. To be more precise, we ask the following question: what is the probability p_σ that a randomly and uniformly chosen momentum belongs to the spectrum of the graph? For example, consider the \mathbb{Z}^1 -periodic graphs of Fig. 1. How does p_σ change if we change the lengths in the fundamental cell of the graph, from Fig. 1(b) to Fig. 1(c)? How does p_σ change if we change the topological structure to Fig. 1(d) or Fig. 1(e)?

Denote by $p_\sigma(K)$ the probability of a uniformly chosen momentum $k \in [0, K]$ to be in the spectrum and let $p_\sigma := \lim_{K \rightarrow \infty} p_\sigma(K)$. We find that the probability p_σ is well defined and is *independent* of many features of the fundamental cell. In particular, all choices in Figs. 1(b)–1(d) lead to the same value of p_σ (assuming a generic choice of edge lengths). This is illustrated by a numerical simulation in Fig. 2. We will derive the limiting value analytically below. Note that the value of p_σ for the cell in Fig. 1(e) turns out to be different from the others and will also be calculated.

Let us put the discussion onto a more formal footing. We consider a \mathbb{Z}^d -periodic network of quantum wires on which we are solving the spectral problem

$$-\frac{d^2 \psi}{dx^2} = k^2 \psi \quad (1)$$

for complex valued functions ψ which are smooth on the edges and subject to the Kirchhoff-Neumann vertex conditions

$$\psi(x) \text{ is continuous at } v \quad \text{and} \quad \sum_{e \in \mathcal{E}_v} \frac{d\psi}{dx_e}(v) = 0, \quad (2)$$

where the sum is over the edges \mathcal{E}_v incident to the vertex v and the derivatives are taken into the edge. We denote by σ the set of k values for which there is a solution to Eqs. (1) and (2); this is the momentum spectrum of the graph. Now, the definition of p_σ can be formally written as

$$p_\sigma = \lim_{K \rightarrow \infty} p_\sigma(K) = \lim_{K \rightarrow \infty} \frac{1}{K} |\sigma \cap [0, K]|. \quad (3)$$

In this Letter, we establish several properties of the probability p_σ . First of all, the above limit always exists. In addition, if there is at least one gap in the spectrum, there are infinitely many gaps and $p_\sigma < 1$. Similarly, if there is at least one nonflat band, there are infinitely many and $p_\sigma > 0$. Finally, and perhaps most strikingly, provided the lengths of edges in the fundamental set are generic, the value of p_σ is *independent* of their precise value. We also find that the value of p_σ is independent of some details of the cell's topology.

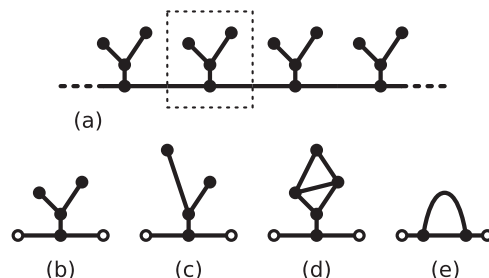


FIG. 1. (a) An example of a \mathbb{Z}^1 -periodic graph and (b) its fundamental cell; (c)–(e) are other examples of the fundamental cell.

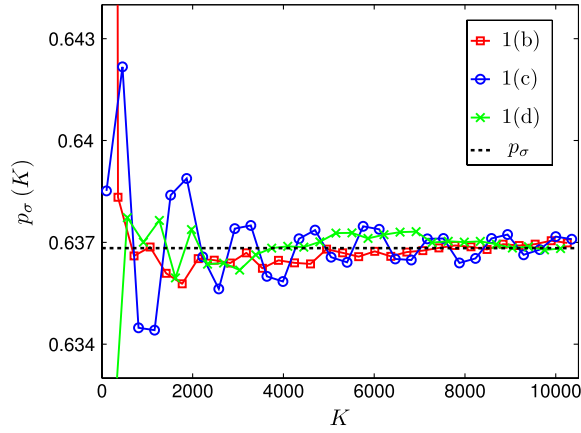


FIG. 2 (color online). Numerical simulation of the convergence of $p_\sigma(K)$ is shown for the three periodic graphs from Figs. 1(b)–1(d). The limiting value p_σ is shown as a dashed line. The graph lengths are normalized such that K equals the average number of spectral bands.

Secular equation and dispersion relation.—In the Floquet-Bloch procedure for quantum graphs (see, e.g., Ref. [7]), we identify a set of d generators of the lattice of periods and assign to each a quasimomentum variable α_j , $j = 1, \dots, d$. If the vertices v_+ and v_- of the fundamental cell are identified by the action of the j th generator, we impose the *quasiperiodic conditions*

$$\psi(v_+) = e^{i\alpha_j} \psi(v_-), \quad \psi'(v_+) = -e^{i\alpha_j} \psi'(v_-). \quad (4)$$

We remind the reader that we use the convention of always taking the derivatives into the edge, which explains the minus sign in conditions (4). For example, in the fundamental cell of Fig. 1(b), the empty circles denote the vertices connected through the condition of the above type. Identifying these periodically related vertices creates new cycles C_j , $j = 1, \dots, d$, on the graph, and the resulting problem is equivalent to a graph with magnetic fluxes α_j through the corresponding cycles. For example, the result of the Floquet-Bloch procedure for the fundamental cell in Fig. 1(d) is equivalent to the *magnetic* graph in Fig. 3(a). We denote by E the number of edges of the resulting magnetic graph.

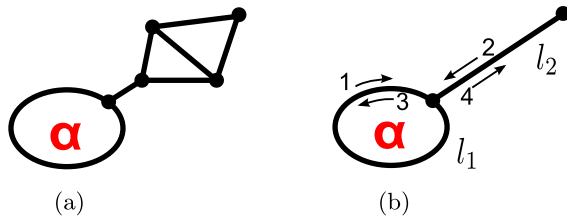


FIG. 3 (color online). (a) A graph consisting of a loop pierced by a magnetic flux and a decoration. (b) Similar graph, but with a single edge decoration.

Expanding the solutions to Eq. (1) for the magnetic graph in the basis of $e^{\pm ikx}$ and applying the vertex conditions leads, after some linear algebra (see Ref. [13]), to the secular equation

$$F(k; \vec{\alpha}) := \det(\mathbf{1} - e^{i(\mathbf{A} + k\mathbf{L})}\mathbf{S}) = 0, \quad (5)$$

where all matrices act in the space of coefficients on directed edges; each edge gives rise to two directed edges of equal length, and therefore all matrices have degree $2E$. The diagonal matrix \mathbf{L} is the matrix of lengths of the directed edges. The diagonal matrix \mathbf{A} contains the magnetic fluxes α_j that are put upon the edges created by vertex identifications. The magnetic fluxes change sign when reversing the direction of the corresponding edge. Finally, the unitary matrix \mathbf{S} contains directed edge-to-edge scattering coefficients, which, for scattering at a Neumann-Kirchhoff vertex of degree d , is equal to $-1 + 2/d$ for backscattering and $2/d$ for forward scattering [see Eqs. (10) and (11), which show these matrices for the graph in Fig. 3(b)]. Most importantly, for our vertex conditions, the matrix \mathbf{S} is independent of k [21].

Next, we apply a clever trick originally due to Barra and Gaspard [22] (see also Ref. [23]): we introduce a new function $\Phi(\vec{k}; \vec{\alpha})$ such that

$$\Phi(\kappa_1 = kl_1, \dots, \kappa_E = kl_E; \vec{\alpha}) := F(k; \vec{\alpha}), \quad (6)$$

where l_1, \dots, l_E are the graph edge lengths. A cursory look at Eq. (5) reveals that the variables κ_e , $e = 1, \dots, E$ need only be known modulo 2π . For a fixed $\vec{\alpha}$, define $\Sigma_{\vec{\alpha}}$ to be the set of solutions of

$$\Phi(\vec{k}; \vec{\alpha}) = 0, \quad (7)$$

on the torus $\mathbb{T}_E := [0, 2\pi)^E$. Then, the roots k_n of the equation $F(k; \vec{\alpha}) = 0$ can be interpreted as the times (k values) of piercing of the set $\Sigma_{\vec{\alpha}}$ by the flow

$$\vec{\kappa}(k) = k(l_1, l_2, \dots, l_E) \bmod 2\pi. \quad (8)$$

We now conclude that k belongs to the spectrum σ of the periodic graph if the corresponding point $\vec{\kappa}(k)$ belongs to the set $\Sigma_{\vec{\alpha}}$ for *some* value of $\vec{\alpha}$ (which itself belongs to a d -dimensional torus). For future purposes, we define

$$\Sigma = \bigcup_{\vec{\alpha} \in [0, 2\pi)^d} \Sigma_{\vec{\alpha}}. \quad (9)$$

We will now compute the set Σ in a simple but important example and then proceed to discuss how the questions about the band probability p_σ can be related to the properties of the set Σ .

Loop with an edge.—Consider the graph which consists of a loop pierced by magnetic field with flux α and a single edge attached; see Fig. 3(b).

The numbering of the directed edges is given in Fig. 3(b). According to this numbering, the matrices \mathbf{A} , \mathbf{L} , and \mathbf{S} are given by

$$\mathbf{A} = \text{diag}(\alpha, 0, -\alpha, 0), \quad \mathbf{L} = \text{diag}(l_1, l_2, l_1, l_2), \quad (10)$$

and

$$\mathbf{S} = \begin{pmatrix} \frac{2}{3} & \frac{2}{3} & -\frac{1}{3} & 0 \\ 0 & 0 & 0 & 1 \\ -\frac{1}{3} & \frac{2}{3} & \frac{2}{3} & 0 \\ \frac{2}{3} & -\frac{1}{3} & \frac{2}{3} & 0 \end{pmatrix}. \quad (11)$$

The secular function Φ evaluates to (up to some nonzero factors)

$$\Phi = 2 \cos(\kappa_2)[\cos(\kappa_1) - \cos(\alpha)] - \sin(\kappa_1) \sin(\kappa_2). \quad (12)$$

The zero sets Σ_α for a range of values of the parameter α are shown in Fig. 4(a). Note that it is enough to consider the values $\alpha \in [0, \pi]$ as $\Sigma_{-\alpha} = \Sigma_\alpha$ [see Eq. (12)].

Probability to be in the spectrum.—From the discussion above, we conclude that the probability p_σ for a random k to be in the spectrum σ is equal to the proportion of time the flow defined by Eq. (8) spends in the set Σ . Depending on the commensurability properties of the set of the edge lengths $\{l_e\}_{e=1}^E$, the flow covers densely the entire torus or is restricted to a flat submanifold

$$\begin{aligned} L &:= \overline{\text{span}[k(l_1, l_2, \dots) \bmod \mathbb{T}_E: k \in \mathbb{R}]} \\ &= \{x \in \mathbb{R}^E: Mx = 0\} \bmod \mathbb{T}_E, \end{aligned}$$

where M is a matrix with rational coefficients [it gives the rational dependencies in the length sequence (l_1, \dots, l_E)]. In the latter case, the flow is ergodic on the submanifold L . The probability p_σ is therefore the relative volume

$$p_\sigma = \frac{\text{vol}_L(L \cap \Sigma)}{\text{vol}_L(L)}, \quad (13)$$

where the subscript L indicates that the volume should be taken in the appropriate dimension (equal to E minus the

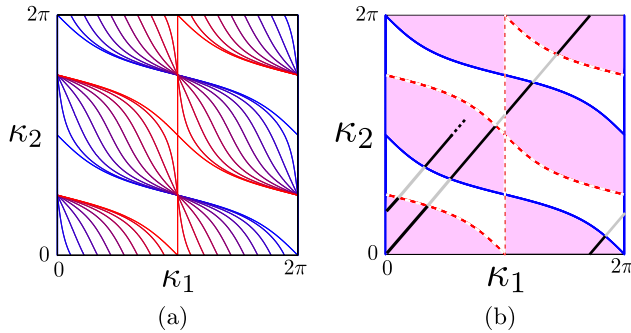


FIG. 4 (color online). (a) The zero sets Σ_α of $\Phi(\kappa_1, \kappa_2; \alpha)$ are shown for a range of values $\alpha \in [0, \pi]$ using a blue ($\alpha = 0$) and red ($\alpha = \pi$) color scale. (b) The set $\Sigma = \bigcup_{\alpha \in [0, 2\pi]} \Sigma_\alpha$ is shaded, its solid blue boundaries are the zeros of $\Phi(\cdot, \cdot; \alpha = 0)$, and the dashed red boundaries are the zeros of $\Phi(\cdot, \cdot; \alpha = \pi)$. A flow $\vec{k}(k) = k(l_1, l_2)$ on the torus is indicated. The bands of the spectrum σ are the solid black segments of the flow line; the gaps are drawn in light gray.

rank of the matrix M). Formula (13) remains valid in the case of rationally independent lengths, when we simply take L to be the entire torus. This immediately implies that the probability p_σ remains the same as long as the edge lengths are rationally independent.

Returning to our example, we calculate p_σ explicitly. Using symmetry, we compute the area of 1/8th of the set Σ , the part in the lower left corner. It is bounded by the coordinate axes and the set Σ_π , which from Eq. (12) we reparametrize as

$$\tan(\kappa_2) = 2 \cot(\kappa_1/2). \quad (14)$$

Therefore, the ratio in Eq. (13) evaluates to

$$p_\sigma = \frac{2}{\pi^2} \int_0^\pi \tan^{-1}[2 \cot(\kappa/2)] d\kappa \approx 0.64. \quad (15)$$

We can further prove that this universality of p_σ extends to a certain class of decoration structures. These are the decorations that attach to the base line by means of a single edge, as in Figs. 1(a)–1(d). Proving the universality is done by reducing the influence of the decoration on the secular equation to a single scattering reflection phase located at the degree one vertex of the graph in Fig. 3(b). The phase enters the matrix \mathbf{S} as follows:

$$\mathbf{S} = \begin{pmatrix} \frac{2}{3} & \frac{2}{3} & -\frac{1}{3} & 0 \\ 0 & 0 & 0 & \Theta(\kappa_3, \dots, \kappa_E) \\ -\frac{1}{3} & \frac{2}{3} & \frac{2}{3} & 0 \\ \frac{2}{3} & -\frac{1}{3} & \frac{2}{3} & 0 \end{pmatrix}. \quad (16)$$

While the precise form of the phase $\Theta(\kappa_3, \dots, \kappa_E)$ may be complicated, its effect on the function Φ gets averaged out by ergodicity. More precisely, we now assume that the rational relations (if any) defining the submanifold L do not involve κ_1 and κ_2 . In other words, the lengths of edges 1 and 2 are rationally independent of each other and of the lengths of the decoration's edges. We need not assume anything about the lengths of edges of the decoration.

One can now easily read from the determinant [see Eqs. (5) and (6)] that the function Φ has the form $\Phi(\kappa_1, \kappa_2, \dots, \kappa_E; \alpha) = \Phi(\kappa_1, \kappa_2 + 1/2\Theta(\kappa_3, \dots, \kappa_E); \alpha)$, where $\Phi(\cdot, \cdot; \alpha)$ in the right-hand side is as in Eq. (12). Introducing the change of variables

$$\hat{\kappa}_2 = \kappa_2 + \frac{1}{2}\Theta(\kappa_3, \dots, \kappa_E), \quad (17)$$

the integrals in Eq. (13) factorize. Namely, denote by \mathbb{T}_2 the torus with respect to κ_1 and $\hat{\kappa}_2$ and by \mathbb{T}_{E-2} the torus with respect to the other variables. Note that the set Σ depends only on the variables κ_1 and $\hat{\kappa}_2$ (and is cylindrical with respect to the other variables). The submanifold L , on the other hand, is cylindrical with respect to κ_1 and $\hat{\kappa}_2$. Therefore,

$$p_\sigma = \frac{\text{vol}_{\mathbb{T}_2}(\mathbb{T}_2 \cap \Sigma) \text{vol}_{\mathbb{T}_{E-2}}(\mathbb{T}_{E-2} \cap L)}{\text{vol}_{\mathbb{T}_2}(\mathbb{T}_2) \text{vol}_{\mathbb{T}_{E-2}}(\mathbb{T}_{E-2} \cap L)}, \quad (18)$$

reducing to the expression in Eq. (13), where L there is identified as \mathbb{T}_2 in Eq. (18). We thus proved that for all decorations of the type discussed above, the probability to be in the spectrum is given by Eq. (15).

To give a final example of a different nature, for the fundamental cell depicted in Fig. 1(e), the secular equation can be shown to be equivalent to

$$\begin{aligned} \sin(\kappa_1 + \kappa_2 + \kappa_3) - \frac{1}{2} \sin \kappa_1 \sin \kappa_2 \sin \kappa_3 \\ = \sin \kappa_1 + \cos \alpha (\sin \kappa_2 + \sin \kappa_3), \end{aligned} \quad (19)$$

and the corresponding value of p_σ was calculated numerically to be 0.43.

Conclusions.—The arguments presented above apply to all graphs and result in three general conclusions. First, given a d -dimensional periodic graph with an arbitrary fundamental cell, the probability p_σ is independent of the specific edge lengths, as long as there are no rational dependencies between some of them. Even if such dependencies exist, the limit (3) which defines p_σ exists and its exact value depends on the nature of the edge length rational dependencies (as well as the graph's topology). Second, we have shown that p_σ is robust even within some topological modifications of the graph—attaching a prescribed class of decorations. Third, if there exists at least one nonflat band (gap) in the spectrum, it must arise from an open set on the torus which is a subset of $\Sigma (\mathbb{T} \setminus \Sigma)$. The ergodic flow on the torus will pass through this set infinitely many times, resulting in an infinite number of nonflat bands (gaps) of comparable size. From Eq. (13), we can immediately conclude that $p_\sigma > 0$ ($p_\sigma < 1$).

Our setup calls for comparison with periodic potentials on the line, in particular, the singular potentials δ and δ' [24]. For smooth periodic potentials and δ potentials, the gap sizes decrease as $k \rightarrow \infty$, while the band lengths converge to a constant, resulting in $p_\sigma = 1$ [25,26]. The δ' potential has an opposite behavior, asymptotically equivalent to disconnecting the graph: the band lengths decrease and the gaps approach a constant size, resulting in $p_\sigma = 0$ [26]. Our results show that a typical nontrivial periodic graph has an intermediate behavior with $0 < p_\sigma < 1$, as long as there is at least one gap and at least one band. This phenomenon can be explained by replacing the decoration with an equivalent scattering matrix. It would be a k -dependent unitary matrix, which oscillates between total reflection and perfect transmission, and therefore emulates the asymptotic behavior of the δ and δ' potentials. This oscillation results in the intermediate values $0 < p_\sigma < 1$. We refer the reader to Refs. [9,27,28] for similar discussions.

One can also consider dressing the network with a bounded periodic potential and/or changing the vertex conditions from the ones we considered. This should not affect our results qualitatively, as the influence of a potential or vertex conditions decreases in the $k \rightarrow \infty$ limit. However, this case is technically more difficult since the

k dependence in Eq. (5) would become more involved. To overcome these difficulties, methods developed in Refs. [29,30] might prove useful.

Some further interesting spectral questions are now within reach. One may obtain bounds on possible sizes of bands (gaps) and deduce the specific edge lengths for which they are attained. Furthermore, the gap opening mechanism, a well studied subject on its own right [31,32], can be better understood by examining the subdomains of the torus which do not intersect Σ . In addition, the topological meaning of p_σ should be further investigated—does it relate to some other graph invariants or does it provide a brand new piece of information on the underlying graph, its periodicity, and the topology of the fundamental cell?

On the more applied side, it is known that the spectrum of quantum graphs is a good approximation of the spectrum of thin branched structures (such as quantum wires or photonic crystals) [33–35]. Intuitively, the approximation remains valid for manifold eigenstates with the first mode in the transversal direction, i.e., for momentum up to $1/\epsilon$, where ϵ is the thickness of the manifold. In this regime, we expect the local density of the continuous spectrum p_σ to be the same as in the graph case. For higher energies, bands corresponding to different transversal modes overlap, and the density of gaps should decrease exponentially with the number of transversal modes present. These heuristic expectations are still to be verified numerically, analytically, and experimentally.

Finally, we make another step forward by extending the discussion to eigenfunction properties. The number of zeros of an eigenfunction was recently found to be connected with the stability of the corresponding eigenvalue with respect to magnetic perturbations [36–38]. The stability is described by the Morse index of the eigenvalue, and most strikingly, this Morse index can be shown to be a well defined function on the torus, not depending on the direction of the flow (i.e., on graph edge lengths) [39]. This leads to new and exciting findings on the distribution of the number of zeros of graph eigenfunctions [40].

We thank D. Cohen, P. Exner, and P. Kuchment for interesting discussions and helpful advice. R. B. acknowledges the support of EPSRC Grant No. EP/H028803/1. G. B. acknowledges the support of NSF Grant No. DMS-0907968. The collaboration between the authors benefited from the support of the EPSRC research network “Analysis on Graphs” (EP/I038217/1).

*ramband@technion.ac.il

†berko@math.tamu.edu

- [1] C. Kittel, *Quantum Theory of Solids* (Wiley, New York, 1963).
- [2] E. Yablonovitch, *Phys. Rev. Lett.* **58**, 2059 (1987).

- [3] J. Zaanen, G. A. Sawatzky, and J. W. Allen, *Phys. Rev. Lett.* **55**, 418 (1985).
- [4] A. Figotin and A. Klein, *SIAM J. Appl. Math.* **58**, 683 (1998).
- [5] C. Luo, M. Ibanescu, S. Johnson, and J. Joannopoulos, *Science* **299**, 368 (2003).
- [6] I. V. Konoplev, L. Fisher, A. W. Cross, A. D. R. Phelps, K. Ronald, and C. W. Robertson, *Appl. Phys. Lett.* **96**, 261101 (2010).
- [7] G. Berkolaiko and P. Kuchment, *Introduction to Quantum Graphs*, Mathematical Surveys and Monographs Vol. 186 (American Mathematical Society, Providence, RI, 2013).
- [8] S. Gnuzmann and U. Smilansky, *Adv. Phys.* **55**, 527 (2006).
- [9] J. E. Avron, P. Exner, and Y. Last, *Phys. Rev. Lett.* **72**, 896 (1994).
- [10] E. Akkermans, A. Comtet, J. Desbois, G. Montambaux, and C. Texier, *Ann. Phys. (N.Y.)* **284**, 10 (2000).
- [11] P. Kuchment and L. Kunyansky, *Adv. Comput. Math.* **16**, 263 (2002).
- [12] P. Kuchment and O. Post, *Commun. Math. Phys.* **275**, 805 (2007).
- [13] T. Kottos and U. Smilansky, *Phys. Rev. Lett.* **79**, 4794 (1997).
- [14] G. Berkolaiko, H. Schanz, and R. S. Whitney, *Phys. Rev. Lett.* **88**, 104101 (2002).
- [15] S. Gnuzmann and A. Altland, *Phys. Rev. Lett.* **93**, 194101 (2004).
- [16] S. Gnuzmann, J. P. Keating, and F. Pietet, *Phys. Rev. Lett.* **101**, 264102 (2008).
- [17] S. Gnuzmann, H. Schanz, and U. Smilansky, *Phys. Rev. Lett.* **110**, 094101 (2013).
- [18] C. H. Joyner, S. Müller, and M. Sieber, [arXiv:1302.2554](https://arxiv.org/abs/1302.2554).
- [19] O. Hul, S. Bauch, P. Pakoński, N. Savytsky, K. Życzkowski, and L. Sirko, *Phys. Rev. E* **69**, 056205 (2004).
- [20] O. Hul, M. Ławniczak, S. Bauch, A. Sawicki, M. Kuś, and L. Sirko, *Phys. Rev. Lett.* **109**, 040402 (2012).
- [21] Therefore, the proof holds for all non-Robin vertex conditions.
- [22] F. Barra and P. Gaspard, *J. Stat. Phys.* **101**, 283 (2000).
- [23] G. Berkolaiko and B. Winn, *Trans. Am. Math. Soc.* **362**, 6261 (2010).
- [24] S. Albeverio, F. Gesztesy, R. Høegh-Krohn, and H. Holden, *Solvable Models in Quantum Mechanics* (American Mathematical Society, Providence, RI, 2005), 2nd ed., with an appendix by Pavel Exner.
- [25] M. I. Weinstein and J. B. Keller, *SIAM J. Appl. Math.* **47**, 941 (1987).
- [26] P. Exner and R. Gawlista, *Phys. Rev. B* **53**, 7275 (1996).
- [27] P. Exner and H. Grosse, [arXiv:math-ph/9910029](https://arxiv.org/abs/math-ph/9910029).
- [28] P. Exner and O. Turek, *J. Phys. A* **43**, 474024 (2010).
- [29] J. Bolte and S. Endres, *Ann. Inst. Henri Poincaré* **10**, 189 (2009).
- [30] R. Rueckriemen and U. Smilansky, *J. Phys. A* **45**, 475205 (2012).
- [31] J. H. Schenker and M. Aizenman, *Lett. Math. Phys.* **53**, 253 (2000).
- [32] P. Kuchment, *J. Phys. A* **38**, 4887 (2005).
- [33] P. Kuchment and H. Zeng, *J. Math. Anal. Appl.* **258**, 671 (2001).
- [34] J. Rubinstein and M. Schatzman, *Arch. Ration. Mech. Anal.* **160**, 271 (2001).
- [35] P. Exner and O. Post, *J. Geom. Phys.* **54**, 77 (2005); see also [arXiv:0706.0481](https://arxiv.org/abs/0706.0481).
- [36] G. Berkolaiko, [arXiv:1110.5373](https://arxiv.org/abs/1110.5373) [Anal. PDE (to be published)].
- [37] Y. Colin de Verdière, [arXiv:1201.1110v2](https://arxiv.org/abs/1201.1110v2) [Anal. PDE (to be published)].
- [38] G. Berkolaiko and T. Weyand, [arXiv:1212.4475](https://arxiv.org/abs/1212.4475) [Phil. Trans. R. Soc. A (to be published)].
- [39] R. Band, [arXiv:1212.6710](https://arxiv.org/abs/1212.6710) [Phil. Trans. R. Soc. A (to be published)].
- [40] R. Band and G. Berkolaiko (to be published).